Dyes and Pigments 86 (2010) 6–14

Contents lists available at ScienceDirect

Dyes and Pigments

journal homepage: www.elsevier.com/locate/dyepig

The synthesis and optical characterization of novel iminocoumarin derivatives

Sheng-Tung Huang [a,*], Jia-Liang Jian [b], Huai-Zu Peng [a], Kun-Li Wang [b], Chun-Mao Lin [c], Chih-Hung Huang [a], Thomas C.-K. Yang [b]

[a] Institute of Biotechnology, National Taipei University of Technology, Taipei, Taiwan
[b] Institute of Chemical Engineering, National Taipei University of Technology, Taipei, Taiwan
[c] College of Medicine, Taipei Medical University, Taipei, Taiwan

ARTICLE INFO

Article history:
Received 10 August 2009
Received in revised form
22 October 2009
Accepted 25 October 2009
Available online 11 November 2009

Keywords:
Iminocoumarins
Benzopyran dyes
Long-wavelength fluorescent dyes
Chromene
Benzimidazole
Near-infrared region dyes

ABSTRACT

A series of novel long-wavelength, fluorescent, novel iminocoumarin derived dyes were synthesized by extending the π-conjugation and spatial location of the benzimidazolic and iminochromene rings in a planar structure. Several dyes display a fluorescent maxima ≥600 nm whilst others showed fluorescent maxima in the NIR region.

1. Introduction

Fluorescence has long been viewed as a powerful tool for basic research in the biological sciences, for instance in the development of new drugs, the assurance of food safety and environmental quality as well as the clinical diagnosis of diseases, owing to its high resolution and sensitivity [1]. Recent breakthroughs in fluorescence microscopy are producing notable improvements in imaging resolution [2,3]. Such technical advances should have a major positive impact on the emerging field of cell imaging using single-molecule methods and help merge the subdisciplines of cell and molecular biology [4,5]. Bright, long-wavelength ($\lambda_{em} > 600$ nm) fluorescent dyes, which emit light in the red or near-infrared (NIR) region, have recently enjoyed interest as luminescent dyes and as fluorescent probes for biomolecules. The demand for fluorescent dyes with a spectral range between 600 and 900 nm has grown [2–5]. Employing long-wavelength dyes in biological imaging significantly reduces the background signal due to the lowest autoabsorption and autofluorescence of biomolecules in the long-wavelength region of the spectrum. In addition, the low light scattering and deep penetration of long-wavelength light required to excite the long-wavelength dyes allows the possibility of using a low-cost excitation light source [6]. However, the full potential of many of these new imaging methods will only be achieved depending upon the availability of suitable dyes.

Fluorescent coumarin derivatives have been widely used in many applications from cell biology, medical analysis, lasers, sensors, to the advanced photophysical systems [7,8]. In contrast, very few reports have been carried out on the neighboring series of iminocoumarin dyes. Of the reported iminocoumarin derivatives, the iminocoumarin moiety has been incorporated as a fluorescence signaling unit in Ca^{2+}, Zn^{2+}, or H^{+} indicators [9–11]. In these reports, the molecular structure of these iminocoumarin moieties incorporate a push-pull functionality, the *N*,*N*-dialkylamino group at the 7-pointion is an electron donor, while an electron withdrawing group, such as the benzimidazole fragment at the 3-position, enhances the fluorescence efficiency [12]. Despite the spectacular successes that have been achieved using coumarin or iminocoumarin derived fluorophores in contemporary pure and applied science; most of these fluorophores illuminate in the blue green region which might limit these dyes for use in biological applications. Many biological samples fluoresce on their own, typically in the blue green region of the spectrum; thus this would interfere with the fluorescence signals generated from the coumarin or iminocoumarin derived fluorophores.

* Corresponding author. Tel.: +886 02 2771 2171; fax: +886 02 2731 7117.
E-mail address: ws75624@ntut.edu.tw (S.-T. Huang).

0143-7208/$ – see front matter © 2009 Elsevier Ltd. All rights reserved.
doi:10.1016/j.dyepig.2009.10.020

The iminocoumarin derived fluorophores are known for their high fluorescence ability and efficient quantum yield [12]. The 3-benzimidazol-2-yl-2-iminocoumarin structure **1** is an extensively employed synthon for the preparation of new fluorophores (Fig. 1). Recently, several groups reported the condensation reaction between the aromatic aldehydes with 3-benzimidazol-2-yl-2-iminocoumarin to produce a rigid molecular structure **2** [13,14], or condensed the same synthon with malononitrile to produce a rigid benzopyran **3** [15] (Fig. 1). However, the fluorescence peaks of both the **2** and **3** structural derivatives still fall short of the long-wavelength region of the spectrum which thus limited their biomedical applications. Our group recently reported the synthesis and evaluation of several 3-benzimidazol-2-yl-2-iminocoumarin derivatives for the dye-sensitized solar cell applications [16]. We were interested in further exploring the chemistry of 3-benzimidazol-2-yl-2-iminocoumarin and have synthesized a series of conformational restricted derivatives i.e. dyes **4**, **5**, **6** and **7** (Fig. 2). We envisioned that the spatial fixation of the benzimidazolic and chromene rings into a planar structure would enhance electron flow within the conjugated ring system. Furthermore, we also introduced various electron withdrawing groups to the C=N group of **3**, **4**, and **5** to enhance the push-pull effect on the molecules. We believed that introducing these structural modifications onto the 3-benzimidazol-2-yl-2-iminocoumarin could create new fluorophores that would emit in the long-wavelength region of the spectrum. In this paper, we report the synthesis of **4**, **5**, **6** and **7** and also the evaluation of their optical properties.

2. Experimental

2.1. Apparatus and chemicals

^{1}H and ^{13}C NMR were obtained on a Bruker AMX-500 spectrometer; chemical shifts are reported in ppm relative to tetramethylsilane (δ units). Electrospray ionization (ESI) was preformed at the Analytical Facility of The National Taiwan University. All chemicals were purchased from Acros, Aldrich or TCI and used without future purification. The iminocoumarin **1a**–**b**, dyes **3a**–**b** and **5a** were prepared according to the published procedures [15–19]. Various phenyl isocyanide dichlorides derivatives were prepared in two steps according to known procedures [20].

2.2. General procedures for preparing dyes ***4a–j***

In a flask fitted with a magnetic stirrer was placed iminocoumarin **1a** (3 mmol), phenyl-isocyanide dichlorides (caution: incompatible with strong oxidizing agents; corrosive) (6 mmol), and isopropanol (5 ml) and then a catalytic amount of piperidine. The resulting reaction mixture was stirred at reflux temperature for 16 h. The precipitate was filtered and purified by recrystallisation with DMF to give **4**.

2.2.1. N,N-Diethyl-7-[(4-nitropheyl)imino]-7H-chromeno [2′, 3′: 4, 5] pyrimido [1, 6-a] benzimidazol-3-amine (***4a***)

Red solid (54% yield) m.p. > 300 °C. FT-IR v/cm^{-1} = 2975, 2929, 2871, 1643, 1596, 1553, 1527, 1505, 1427, 1333, 1266, 1234, 1204, 1181, 1135, 1113, 1080, 1005 cm^{-1}. ^{1}H NMR (500 MHz, $CDCl_3$): δ = 8.71 (d, J = 7.9 Hz, 1H), 8.67 (s, 1H), 8.28 (d, J = 8.9 Hz, 2H), 7.85 (d, J = 7.9 Hz, 1H), 7.51–7.42 (m, 3H), 7.38 (d, J = 8.9 Hz, 2H), 6.76 (dd, J = 9.0, 2.3 Hz, 1H), 6.68 (d, J = 2.3 Hz, 1H), 3.49 (q, J = 7.1 Hz, 4H), 1.27 (t, J = 7.1 Hz, 6H). ^{13}C NMR (125 MHz, $CDCl_3$): δ = 162.1, 156.3, 155.0, 153.3, 145.7, 145.0, 144.6, 143.4, 136.9, 131.2, 131.1, 125.1, 124.7, 124.0, 123.8, 118.9, 116.6, 111.4, 110.3, 104.3, 97.5, 45.4, 12.4. HRMS-ESI (m/z): [M + 1] For $C_{27}H_{22}N_6O_3$, 478.1753 calcd; 479.1855 found.

2.2.2. N,N-Dibutyl-7-[(4-nitropheyl) imino]-7H-chromeno [2′, 3′: 4, 5] pyrimido [1, 6-a] benzimidazol-3-amine (***4b***)

Red solid (61% yield) m.p. 244–246 °C. FT-IR v/cm^{-1} = 2957, 2929, 2871, 1639, 1595, 1553, 1525, 1505, 1484, 1421, 1332, 1276, 1218, 1136, 1111, 1097 cm^{-1}. ^{1}H NMR (500 MHz, $CDCl_3$): δ = 8.70 (d, J = 8.0 Hz, 1H), 8.66 (s, 1H), 8.28 (d, J = 8.9 Hz, 2H), 7.84 (d, J = 8.0 Hz, 1H), 7.49–7.41 (m, 3H), 7.38 (d, J = 8.9 Hz, 2H), 6.72 (dd, J = 9.0, 2.2 Hz, 1H), 6.63 (d, J = 2.2 Hz, 1H), 3.39 (t, J = 7.8 Hz, 4H), 1.66–1.60 (t, J = 7.2, 4H), 1.43–1.36 (m, 4H), 0.99 (t, J = 7.3 Hz, 6H). ^{13}C NMR (125 MHz, $CDCl_3$): δ = 162.1, 156.2, 155.0, 153.7, 145.7, 144.9, 143.4, 136.9, 131.2, 130.9, 125.1, 124.7, 124.0, 123.7, 118.9, 116.6, 111.5, 110.3, 104.1, 97.6, 51.5, 29.3, 20.2, 13.9. HRMS-ESI (m/z): [M + 1] For $C_{31}H_{30}N_6O_3$, 534.2379 calcd; 535.2457 found.

2.2.3. 4-{[3-Diethylamino]-7H-chromeno [2′, 3′: 4, 5] pyrimidol [1, 6-a] benzimidazol-7-ylidene] amino} benzonitrile (***4c***)

Red solid (65% yield) m.p. > 300 °C. FT-IR v/cm^{-1} = 2974, 2932, 2870, 2214, 1631, 1603, 1555, 1524, 1508, 1492, 1424, 1338, 1276, 1264, 1232, 1200, 1184, 1167, 1133, 1112, 1080, 1012 cm^{-1}. ^{1}H NMR (500 MHz, $CDCl_3$): δ = 8.71 (d, J = 8.0 Hz, 1H), 8.66 (s, 1H), 7.85 (d, J = 8.0 Hz, 1H), 7. 67(d, J = 8.4 Hz, 2H), 7.51–7.41 (m, 3H), 7.35 (d, J = 8.4 Hz, 2H), 6.75 (dd, J = 9.1, 2.3 Hz, 1H), 6.68 (d, J = 2.3 Hz, 1H), 3.49 (q, J = 7.1 Hz, 4H), 1.27 (t, J = 7.1 Hz, 6H). ^{13}C NMR (125 MHz, $CDCl_3$): δ = 162.0, 156.2, 153.2, 152.7, 145.7, 144.8, 144.6, 136.7, 132.8, 131.3, 131.0, 125.0, 124.1, 124.0, 120.0, 118.9, 116.7, 111.3, 110.3, 105.9, 104.5, 97.5, 45.4, 29.7, 12.4. HRMS-ESI (m/z): [M + 1] For $C_{28}H_{22}N_6O$, 458. 1855 calcd; 459.1975 found.

2.2.4. 4-{[3-Dibutylamino]-7H-chromeno [2′, 3′: 4, 5] pyrimidol [1, 6-a] benzimidazol-7-ylidene] amino} benzonitrile (***4d***)

Red solid (65% yield) m.p. 256–258 °C. FT-IR v/cm^{-1} = 2957, 2931, 2870, 2218, 1636, 1601, 1554, 1527, 1507, 1443, 1421, 1338, 1291, 1273, 1256, 1218, 1168, 1135, 1112, 1096 cm^{-1}. ^{1}H NMR (500 MHz, $CDCl_3$): δ = 8.71 (d, J = 7.9 Hz, 1H), 8.65 (s, 1H), 7.84 (d, J = 7.9 Hz, 1H), 7. 67 (d, J = 8.4 Hz, 2H), 7.49–7.41 (m, 3H), 7.35 (d, J = 8.4 Hz, 2H), 6.72 (dd, J = 9.0, 2.2 Hz, 1H), 6.64 (d, J = 2.2 Hz, 1H), 3.39 (t, J = 7.4 Hz, 4H), 1.66–1.60 (m, 4H), 1.44–1.36 (m, 4H), 0.99 (t, J = 7.3 Hz, 6H). ^{13}C-NM (125 MHz, $CDCl_3$): δ = 162.1, 156.2, 153.6, 152.7, 145.7, 144.8, 144.6, 136.7, 132.9, 131.3, 130.9, 125.0, 124.1, 124.0, 118.9, 116.7, 111.4, 110.2, 104.3, 97.7, 51.5, 29.3, 20.2, 13.9.

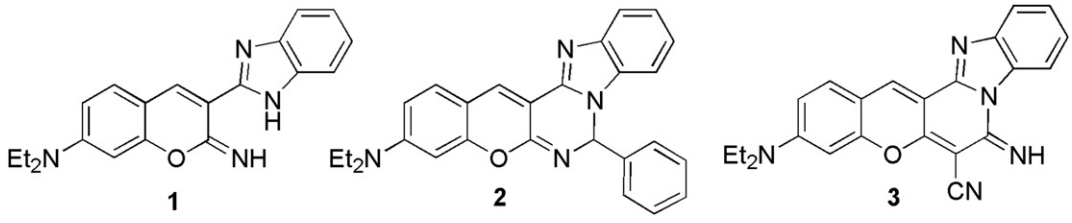

Fig. 1. Chemical structural of **1**, **2**, and **3**.

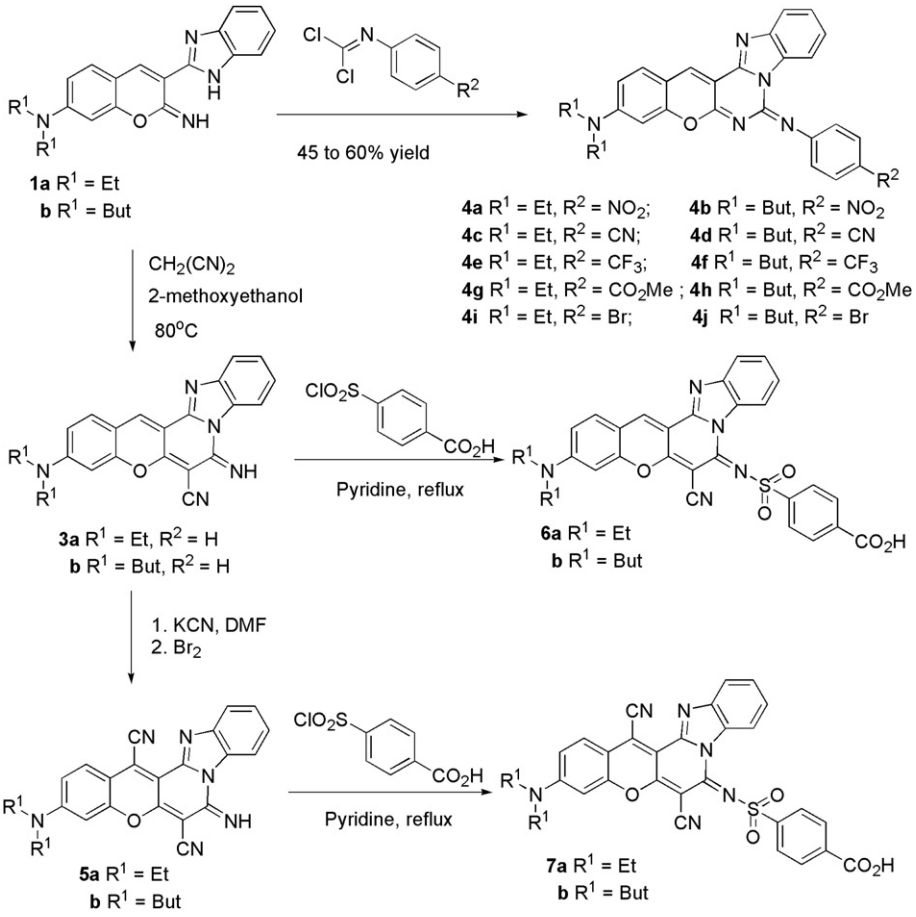

Fig. 2. Synthetic schemes for dyes **4a**–**j**, **5a**–**b**, **6a**–**b**, and **7a**–**b**.

HRMS-ESI (m/z): [M + 1] For $C_{32}H_{30}N_6O$, 514.2481 calcd; 515.2577 found.

*2.2.5. N,N-Diethyl-7-[(4-trifluoromethyl)imino]-7H-chromeno [2′, 3′: 4, 5] pyrimido [1, 6-a] benzimidazol-3-amine (**4e**)*

Red solid (55% yield) m.p. > 300 °C. FT-IR v/cm^{-1} = 2973, 2932, 2873, 1641, 1607, 1557, 1528, 1507, 1444, 1422, 1324, 1264, 1231, 1202, 1180, 1133, 1111, 1034, 1013 cm^{-1}. ^{1}H NMR (500 MHz, $CDCl_3$): δ = 8.74 (d, J = 7.8 Hz, 1H), 8.65 (s, 1H), 7.84 (d, J = 7.8 Hz, 1H), 7. 64 (d, J = 8.3 Hz, 2H), 7.49–7.40 (m, 3H), 7.36 (d, J = 8.3 Hz, 2H), 6.71 (d, J = 10.2 Hz, 1H), 6.66 (s, 1H), 3.47 (q, J = 7.1 Hz, 4H), 1.25 (t, J = 7.1 Hz, 6H). ^{13}C NMR (125 MHz, $CDCl_3$): δ = 161.8, 156.2, 153.2, 151.3, 145.7, 144.4, 144.1, 136.7, 131.3, 131.0, 125.9, 125.8, 125.0, 124.9, 124.0, 123.3, 118.7, 116.7, 111.1, 110.2, 104.2, 97.5, 45.4, 12.4. HRMS-ESI (m/z): [M + 1] For $C_{28}H_{22}F_3N_5O$, 501.1776 calcd; 502.1899 found.

*2.2.6. N,N-Dibutyl-7-[(4-trifluoromethyl)imino]-7H-chromeno [2′, 3′: 4, 5] pyrimido [1, 6-a] benzimidazol-3-amine (**4f**)*

Red solid (61% yield) m.p. 288–290 °C. FT-IR v/cm^{-1} = 2956, 2930, 2873, 1638, 1605, 1557, 1529, 1506, 1420, 1323, 1290, 1277, 1218, 1136, 1111, 1064, 1013 cm^{-1}. ^{1}H NMR (500 MHz, $CDCl_3$): δ = 8.74 (d, J = 7.9 Hz, 1H), 8.61 (s, 1H), 7.84 (d, J = 7.9 Hz, 1H), 7.64(d, J = 8.3 Hz, 2H), 7.47–7.40 (m, 3H), 7.35 (d, J = 8.3 Hz, 2H), 6.70 (dd, J = 8.9, 2.2 Hz, 1H), 6.62 (d, J = 2.2 Hz, 1H), 3.38 (t, J = 7.8 Hz, 4H), 1.65–1.59 (t, J = 7.2 Hz, 4H), 1.43–1.35 (m, 4H), 0.99 (t, J = 7.4 Hz, 6H). ^{13}C NMR (125 MHz, $CDCl_3$): δ = 161.9, 156.1, 153.5, 151.4, 145.7, 144.6, 144.5, 136.4, 131.4, 130.8, 125.9, 125.8, 125.1, 124.9, 123.9, 123.7, 123.3, 118.8, 116.7, 111.2, 110.1, 104.4, 97.7, 51.5, 29.3, 20.3, 13.9. HRMS-ESI (m/z): [M + 1] For $C_{32}H_{30}F_3N_5O$, 557.2402 calcd; 558.2501 found.

*2.2.7. Methyl 4-{[3-diethylamino]-7H-chromeno [2′, 3′: 4, 5] pyrimidol [1, 6-a] benzimidazol-7-ylidene] amino} benzoate (**4g**)*

Red solid (68% yield) m.p. > 300 °C. FT-IR v/cm^{-1} = 2968, 2924, 2853, 1713, 1638, 1603, 1581, 1552, 1525, 1509, 1423, 1336, 1269, 1232, 1200, 1180, 1132, 1111, 1098, 1045, 1012 cm^{-1}. ^{1}H NMR (500 MHz, $CDCl_3$): δ = 8.74 (d, J = 7.8 Hz, 1H), 8.59 (s, 1H), 8.08 (d, J = 8.5 Hz, 2H), 7.83 (d, 7.8 Hz, 1H), 7.46–7.39 (m, 3H), 7.33 (d, J = 8.5 Hz, 2H), 6.69 (dd, J = 9.0, 2.3 Hz, 1H), 6.62 (d, J = 2.3 Hz, 1H), 3.92 (s, 3H), 3.44 (q, J = 7.1 Hz, 4H), 1.24 (t, J = 7.1 Hz, 6H). ^{13}C NMR (500 MHz, $CDCl_3$): δ = 167.4, 161.7, 156.1, 153.0, 152.8, 145.7, 144.5, 144.3, 136.3, 131.4, 130.9, 130.5, 124.8, 124.7, 123.9, 123.1, 118.8, 116.7, 111.0, 110.1, 104.5, 97.5, 51.8, 45.3, 12.4. HRMS-ESI (m/z): [M + 1] For $C_{29}H_{25}N_5O_3$, 491.1957 calcd; 492.2042 found.

*2.2.8. Methyl 4-{[3-dibutylamino]-7H-chromeno [2′, 3′: 4, 5] pyrimidol [1, 6-a] benzimidazol-7-ylidene] amino} benzoate (**4h**)*

Red solid (61% yield) m.p. 235–237 °C. FT-IR v/cm^{-1} = 2956, 2928, 2871, 1712, 1635, 1602, 1557, 1525, 1506, 1423, 1363, 1335, 1277, 1218, 1176, 1135, 1111, 1046, 1015, 822 cm^{-1}. ^{1}H NMR (500 MHz, $CDCl_3$): δ = 8.74 (d, J = 7.9 Hz, 1H), 8.60 (s, 1H), 8.08 (d, J = 8.5 Hz, 2H), 7.83 (d, 7.9 Hz, 1H), 7.47–7.40 (m, 3H), 7.32 (d, J = 8.5 Hz, 2H), 6.67 (dd, J = 9.0, 2.2 Hz, 1H), 6.59 (d, J = 2.2 Hz, 1H), 3.92 (s, 3H), 3.36 (t, J = 7.8 Hz, 4H), 1.63–1.58 (t, J = 7.4 Hz, 4H), 1.42–1.34 (m, 4H), 0.98 (t, J = 7.4 Hz, 6H). ^{13}C NMR (500 MHz, $CDCl_3$): δ = 167.4, 161.8, 156.1, 153.4, 152.8, 145.7, 144.6, 144.3, 136.2, 131.4, 130.7, 130.5, 124.8, 124.7, 123.9, 123.1, 118.8, 116.7, 111.1, 110.1,

104.5, 97.7, 51.8, 51.4, 29.3, 20.2, 13.8. HRMS-ESI (m/z): [M + 1] For $C_{33}H_{33}N_5O_3$, 547.2583 calcd; 548.2705 found.

*2.2.9. N,N-Diethyl-7-[(4-bromophenyl)imino]-7H-chromeno [2′, 3′: 4, 5] pyrimido [1, 6-a] benzimidazol-3-amine (**4i**)*

Red solid (68% yield) m.p. 290–292 °C. FT-IR v/cm^{-1} = 2971, 2928, 2868, 1637, 1590, 1556, 1526, 1510, 1480, 1421, 1339, 1264, 1231, 1185, 1133, 1112, 1097, 1077, 1005 cm^{-1}. ^{1}H NMR (500 MHz, $CDCl_3$): δ = 8.75 (d, J = 7.7 Hz, 1H), 8.60 (s, 1H), 7.83 (d, J = 7.7 Hz, 1H), 7.49 (d, J = 8.5 Hz, 2H), 7.50–7.40 (m, 3H), 7.21 (d, J = 8.5 Hz, 2H), 6.72 (dd, J = 9.0, 2.3 Hz, 1H), 6.66 (d, J = 2.3 Hz, 1H), 3.48 (q, J = 7.1 Hz, 4H), 1.26 (t, J = 7.1 Hz, 6H). ^{13}C NMR (500 MHz, $CDCl_3$): δ = 161.6, 156.1, 153.0, 147.0, 144.2, 136.0, 131.6, 131.5, 130.8, 125.2, 124.8, 123.9, 118.8, 116.8, 116.4, 110.9, 110.1, 104.8, 97.6, 45.4, 29.7, 18.3, 12.4. HRMS-ESI (m/z): [M + 1] For $C_{27}H_{22}BrN_5O$, 511.1008, 513.0987 calcd; 512.1101, 514.1080 found.

*2.2.10. N,N-Dibutyl-7-[(4-bromophenyl)imino]-7H-chromeno [2′, 3′: 4, 5] pyrimido [1, 6-a] benzimidazol-3-amine (**4j**)*

Red solid (68% yield) m.p. 232–234 °C. FT-IR v/cm^{-1} = 2956, 2930, 2872, 1634, 1591, 1553, 1529, 1509, 1481, 1420, 1341, 1273, 1249, 1219, 1130, 1111, 1068, 1007. ^{1}H NMR (500 MHz, $CDCl_3$): δ = 8.75 (d, J = 7.8 Hz, 1H), 8.61 (s, 1H), 7.83 (d, J = 7.8 Hz, 1H), 7.49 (d, J = 8.5 Hz, 2H), 7.46–7.39 (m, 3H), 7.21 (d, J = 8.5 Hz, 2H), 6.68 (dd, J = 8.9, 2.3 Hz, 1H), 6.61 (d, J = 2.3 Hz, H), 3.37 (t, J = 7.8 Hz, 4H), 1.65–1.59 (t, J = 7.2 Hz, 4H), 1.43–1.36 (m, 4H), 0.99 (t, J = 7.4 Hz, 6H). ^{13}C NMR (500 MHz, $CDCl_3$): δ = 161.6, 156.0, 153.4, 147.0, 145.7, 144.2, 136.2, 131.6, 131.4, 130.8, 125.2, 124.8, 123.9, 118.7, 116.8, 116.4, 111.1, 110.1, 104.4, 97.7, 51.4, 29.7, 29.3, 20.2, 13.9. HRMS-ESI (m/z): [M + 1] For $C_{31}H_{30}BrN_5O$, 567.1634, 569.1613 calcd; 568.1765, 570.1701 found.

*2.3. Procedures for preparing 3-(dibutylamino)-7-imino-7H-chromeo[3′, 2′: 3, 4] pyrido [1, 2-a] benzimidazole-6-carbonitrile (**3b**)*

To a solution of **1b** (1 mmol) in 3 ml dry 2-methoxyethanol was added malononitrile (1 mmol), and the solution was stirred 80 °C for 4 h. The mixture was cooled to room temperature and the red coloured precipitate was filtered and purified by recrystallisation with DMF to give **3b** as red solid (68% yield). M.p. 296–299 °C. FT-IR v/cm^{-1} = 3333, 3190, 2957, 2208, 1356, 1276, 1222, 1169, 1124. ^{1}H NMR (500 MHz, DMSO-d_6): δ = 8.76 (d, J = 7.6 Hz, 1H), 8.05 (s, 1H), 8,41 (br, 1H, NH), 7.80 (d, J = 7.6 Hz, 1H,), 7.42 (m, 3H), 6.68 (dd, J = 9.0, 2.1 Hz, 1H), 6.63 (s, 1H), 3.41 (t, J = 7.9 Hz 4H,), 1.65 (m, 4H), 1.46–1.39 (m, 4H), 1.25–0.98 (m, 6H). HRMS-ESI (m/z): [M] For $C_{27}H_{27}N_5O$, 437.2216 calcd; 437.2230 found.

*2.4. General preparation of **5a** and **5b***

To a solution of **5** (20 mmol) in 50 ml of DMF was added potassium cyanide (40 mmol in 6 ml of water). The solution was stirred at 40 °C for 1 h, cooled to room temperature and filtered. After filtration, 20 mmol of elemental bromine was added dropwise to the filtrate at 0 °C and the ensuing mixture was stirred for an additional 60 min at this temperature. The resulting precipitate was collected, washed with water and methanol and purified by double recrystallisation from DMF.

*2.4.1. 3-(Diethylamino)-7-imino-7H-chromeno [3′, 2′: 3, 4] pyrido [1, 2-a] benzimidazole-6, 14-dicarbonitrile (**5a**)*

Deep blue solid (70% yield) m.p. > 300 °C. FT-IR v/cm^{-1} = 3293, 2978, 2213, 1643, 1599, 1533, 1504, 1475, 1434, 1334, 1310, 1289, 1260, 1185, 1151, 1111, 1079, 1015. ^{1}H NMR (500 MHz, acetic acid-d_4): δ = 8.06 (d, J = 9.2 Hz, 1H), 7.99 (d, J = 7.6 Hz, 1H), 7.62 (t, J = 7.6 Hz, 1H), 7.56 (t, J = 7.6 Hz, 1H), 7.39 (d, J = 9.2 Hz, 1H), 7.18 (s, 1H), 3.76 (q, J = 7.0 Hz, 4H), 1.33 (t, J = 7.0 Hz, 6H). HRMS-ESI (m/z): [M + 1] For $C_{24}H_{18}N_6O$, 406.1542 calcd; 407.1598 found.

*2.4.2. 3-(Dibutylamino)-7-imino-7H-chromeno [3′, 2′: 3, 4] pyrido [1, 2-a] benzimidazole-6, 14-dicarbonitrile (**5b**)*

Deep blue solid (77% yield) m.p. > 300 °C. FT-IR v/cm^{-1} = 3305, 2956, 2928, 2871, 2217, 1666, 1621, 1601, 1547, 1508, 1445, 1425, 1359, 1340, 1306, 1278, 1225, 1186, 1153, 1110, 1074. ^{1}H NMR (500 MHz, $CDCl_3$): δ = 8.69 (s, 2H), 7.92 (dd, J = 6.9, 2.3 Hz, 1 H), 7.76 (d, J = 9.2 Hz, 1H), 7.46–7.43 (m, 2H), 6.74 (dd, J = 9.2, 2.3 Hz, H), 6.58 (d, J = 2.3 Hz, 1H), 3.43 (t, J = 7.9 Hz, 4H), 1.66 (t, J = 7.1, 4H), 1.47–1.40 (m, 4H), 1.03–1.00 (t, J = 7.4 Hz, 6H). HRMS-ESI (m/z): [M + 1] For $C_{28}H_{26}N_6O$, 462.2186 calcd; 463.2253 found.

*2.5. General procedures for preparation of **6a–b** and **7a–b***

In a flask fitted with a magnetic stirrer placed 2.6 mmol of either **3a–b** or **5a–b**, and 26 ml of dry pyridine and heated up to 120 °C under an argon atmosphere. At 120 °C, 4-chlorosulfonyl-benzoic acid (10 mmol) was added and the ensuing mixture was stirred overnight. The pyridine in the mixture was removed under reduced pressure to yield the crude oily product which was added 10 ml of 2 M aq HCl to give blue precipitate. The resulting crude precipitate was collected, washed with water and methanol and purified by flash column chromatography (1:25/MeOH: CH_2Cl_2).

*2.5.1. 4-({6-Cyano-3-(diethylamino)-7H-chromeno[3′, 2′: 3, 4] pyrido [1, 2-a] benzimidazol-7-ylidene} amino) sulfonyl benzoic acid (**6a**)*

Deep blue solid (43% yield) m.p. > 300 °C. FT-IR v/cm^{-1} = 3456, 1614, 1551, 1502, 1465, 1346, 1295, 1182, 1130, 1038, 1010. ^{1}H NMR (500 MHz, DMSO-d_6): δ = 9.04 (s, 1H), 8.53 (d, J = 8.5 Hz, 1H), 8.0 (d, J = 7.0 Hz, 2H), 7.91 (d, J = 9.5 Hz 1H), 7.84 (d, J = 7.6 Hz, 1H), 7.70 (d, J = 7.0 Hz, 2H), 7.50 (t, J = 7.6 Hz, 1H), 7.53 (t, J = 7.6 Hz, 1H), 7.11 (d, J = 9.5 Hz, 2H), 6.87 (s, 1H), 3.61 (q, J = 7.0 Hz, 4H), 1.19 (t, J = 7.0 Hz, 6H). HRMS-ESI (m/z): [M − 1] For $C_{30}H_{23}N_5O_5S$, 565.1420 calcd; 564.1341 found.

*2.5.2. 4-({6-Cyano-3-(dibutylamino)-7H-chromeno[3′, 2′: 3, 4] pyrido [1, 2-a] benzimidazol-7-ylidene} amino) sulfonyl) benzoic acid (**6b**)*

Deep blue solid (51% yield) m.p. > 300 °C. FT-IR v/cm^{-1} = 3452, 2955, 2214, 1640, 1549, 1505, 1471, 1338, 1287, 1222, 1172, 1128, 1037, 1009. ^{1}H NMR (500 MHz, DMSO-d_6): δ = 9.04 (s, 1H), 8.52 (d, J = 8.3 Hz, 1H), 8.01 (d, J = 8.3 Hz, 2H), 7.90 (d, J = 9.2 Hz, 1H), 7.83 (d, J = 8.2 Hz, 1H), 7.71 (d, J = 8.3 Hz, 2H), 7.48 (t, J = 8.2 Hz, 1H), 7.42 (t, J = 8.3 Hz, 1H), 7.09 (d, J = 9.2 Hz, 1H), 6.84 (s, 1H) 3.53 (t, J = 7.4 Hz, 4H), 1.56–1.55 (m, 4H), 1.35 (m, 4H), 0.92 (t, J = 7.3 Hz, 6H). HRMS-ESI (m/z): [M − 1] For $C_{34}H_{31}N_5O_5S$, 621.2046 calcd; 620.1971 found.

*2.5.3. 4-({6, 14-Dicyano-3-(diethylamino)-7H-chromeno[3′, 2′: 3, 4] pyrido [1, 2-a] benzimidazol-7-ylidene} amino) sulfonyl benzoic acid (**7a**)*

Deep blue solid (42% yield) m.p. > 300 °C. FT-IR v/cm^{-1} = 3446, 2924, 1607, 1547, 1445, 1335, 1232, 1186, 1109, 1035, 1007. ^{1}H NMR (500 MHz, DMSO-d_6): δ = 8.51 (d, J = 8.0 Hz, 1H), 7.99 (d, J = 8.0 Hz, 1H), 7.93 (d, J = 7.6 Hz, 1H), 7.79 (d, J = 9.2 Hz, 2H), 7.72 (d, J = 8.0 Hz, 2H), 7.54–7.49 (m, 2H), 7.22 (d, J = 9.2 Hz, 1H), 6.92 (s, 1H), 3.64 (q, J = 7.1 Hz, 4H), 1.20 (t, J = 7.1 Hz, 6H). HRMS-ESI (m/z): [M − 1] For $C_{31}H_{22}N_6O_5S$, 590.1372 calcd; 589.1298 found.

*2.5.4. 4-({6, 14-Dicyano-3-(dibutylamino)-7H-chromeno[3′, 2′: 3, 4] pyrido [1, 2-a] benzimidazol-7-ylidene} amino) sulfonyl benzoic acid (**7b**)*

Deep blue solid (48% yield) m.p. > 300 °C. FT-IR v/cm^{-1} = 3447, 2927, 2218, 1634, 1466, 1440, 1338, 1283, 1221, 1181, 1110, 1036, 1007. ^{1}H NMR (500 MHz, DMSO-d$_6$, 350K): δ = 8.52 (d, J = 8.2 Hz, 1H), 7.97 (d, J = 8.2 Hz, 2H), 7.92 (d, J = 7.4 Hz, 1H), 7.80 (d, J = 9.4 Hz, 2H), 7.75 (d, J = 8.2 Hz, 2H), 7.55 (m, 2H), 7.19 (d, J = 9.4 Hz, 1H), 6.85 (s, 1H), 3.59 (t, J = 7.3 Hz, 4H), 1.61 (m, 4H), 1.41–1.36 (m, 4H), 0.94 (t, J = 3.7 Hz, 6H). HRMS-ESI (m/z): [M − 1] For $C_{35}H_{30}N_6O_5S$, 646.1998 calcd; 645.1931 found.

2.6. Optical measurement

Absorption spectra were recorded on a Perkin-Elmer spectrophotometer. The all fluorescence measurements were made with using a fluorescence grade quartz cuvette, and a Horiba Jobin Yvon FluoroMax-4 spectrofluorometer. The fluorescence quantum yields of the new dyes were determined by comparisons with reference compound with known quantum yield, and the experimental procedures were performed by following the published procedure [21]. The following reference dyes were used: crystal violet (ϕ = 0.54 in methanol) [22] for **4a**–**j**, **3a**–**b** and **6a**–**b**, zinc phthalocyanine (ϕ = 0.30 in 1% pyridine in toluene) for **5a**–**b**, and **7a**–**b** [23].

3. Results and discussion

3.1. Syntheses of dyes

The synthetic schemes of the new dyes **4**, **5**, **6** and **7** are outlined in Fig. 2. The new dyes **4a**–**j** prepared in one step from 3-benzimidazol-2-yl-2-imunocoumarin **1a** or **1b** [12]. Thus treatment of the iminocoumarin **1a** and **1b** with various *p*-substituted phenyl isocyanide dichlorides [20] in isopropanol under piperidine catalysis resulted in formation of the guanidine dyes **4a**–**j** in 45–60% yields (Fig. 2). The rigid benzopyran ring structure of **3a** and **b** were prepared in one step from the corresponding 3-benzimidazol-2-yl-2-imunocoumarin **1a** or **1b** by condensing with malononitrile following a previously published procedure [15]. Nucleophilic addition of the nitrile to the chromene ring structure of **3a** and **b** followed by bromine oxidation gave **5a** and **5b** in 70% and 77% yields, respectively [24]. The treatment of either **3a**–**b** or **5a**–**b** with 4-carboxybenzenesulfonyl chloride gave the sulfonamide in **6a**–**b** or **7a**–**b**, respectively. The chemical structures of the newly synthesized iminocoumarin derivatives were characterized by NMR, IR and mass; all of the characterization data are listed in the Experimental section. We believe that compounds **4** should possess the *E* stereochemistry, and we assumed compounds **6** and **7** will possess *Z* stereochemistry on steric grounds. However, there is no direct evidence at this point for these stereochemical assignments. Experiments to assist with the elucidation of the stereochemistry of these dyes are presently ongoing.

3.2. Spectral characteristics of the dyes *4a–j*

The basic spectral characteristics of **4a**–**j**, such as the absorption maxima (λ_{max}) and emission maxima (λ_{em}), were measured in dimethyl sulfoxide (DMSO) and the results are presented in Table 1 and Figs. 3–6. In general, the absorption and fluorescence spectra characteristics for dyes **4a**–**j**, which have the same R^2 substituents, exhibited nearly identical spectra for either *N*-ethyl or *N*-butyl substitutions (Table 1 and Figs. 3–6). The electron absorption spectra of dyes **4a**–**j** displayed absorptions in the visible region from 450 nm to 600 nm with one absorption maxima between 529 and 536 nm depending on the different electron withdrawing group (Figs. 3 and 4). The fluorescence spectra of dyes **4a**–**j** displayed emission spectra in the visible region from 500 nm to 700 nm with one emission maxima between 573 and 601 nm also depending on the nature of the electron withdrawing group (Figs. 5 and 6). We observed a drastic bathochromic shift in both the absorption and emission maxima for dyes **4a**–**j** as compared to iminocoumarin **1**. We believe that this bathochromic shift in the spectra results from the extension of the π-conjugation and the spatial fixation of the benzimidazole unit with the C=N bond of the iminochromene bicycle into the planar guanidine structure thereby enhancing the electron flow within the conjugation ring system.

Table 1
Spectroscopic data of the synthesized dyes measured in DMSO at room temperature.

Dyes	λ_{abs} (nm)	λ_{flu} (nm)	ε (M^{-1} cm^{-1})	Stokes shift	ϕ[a]
1a	437	497	41 318	60	0.37
4a	536	600	56 667	64	8.8 E^{-3}
4b	538	601	53 297	63	9.1 E^{-3}
4c	532	580	61 802	48	5.4 E^{-3}
4d	535	583	51 192	48	5.7 E^{-3}
4e	530	573	60 544	43	6.5 E^{-3}
4f	532	576	54 455	44	6.5 E^{-3}
4g	531	581	47 428	50	3.8 E^{-3}
4h	532	576	35 658	44	3.5 E^{-3}
4i	529	561	42 869	32	3.2 E^{-3}
4j	533	561	43 177	32	4.2 E^{-3}
3a	551	577	23 498	26	0.92
3b	553	580	23 732	27	0.94
5a	640	689	32 148	49	0.19
5b	642	694	30 105	52	0.17
6a	570	607	18 128	37	0.90
6b	571	610	41 160	39	0.89
7a	673	715	12 842	42	0.11
7b	676	720	20 613	44	0.12

[a] Reference dyes are listed in the Experimental section.

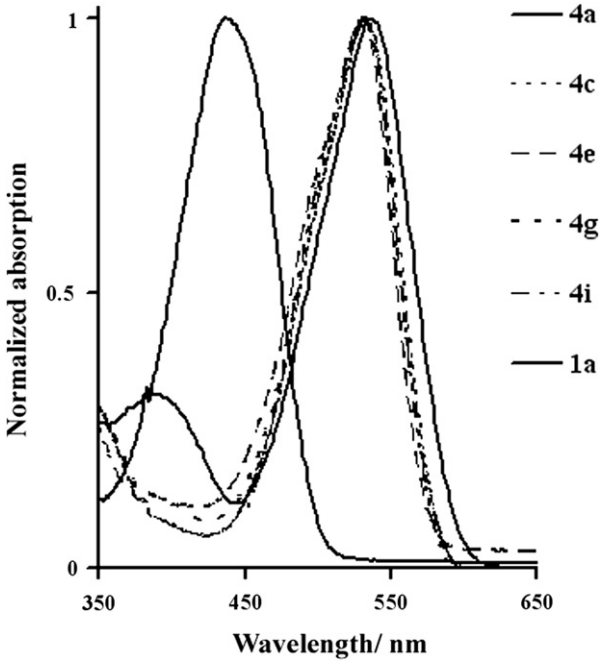

Fig. 3. Normalized absorption spectra for dyes **4a**, **4c**, **4e**, **4g**, **4i**, and **1a** in dimethyl sulfoxide.

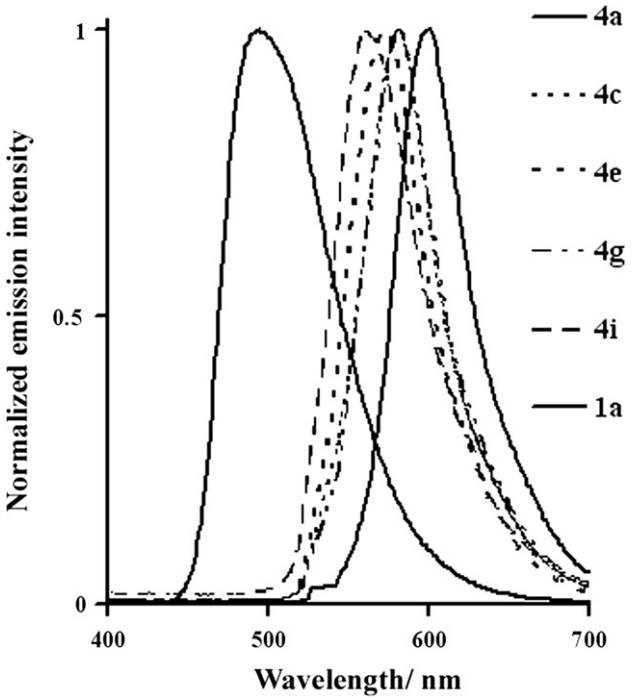

Fig. 4. Normalized fluorescence spectra for dyes **4a**, **4c**, **4e**, **4g**, **4i**, and **1a** in dimethyl sulfoxide.

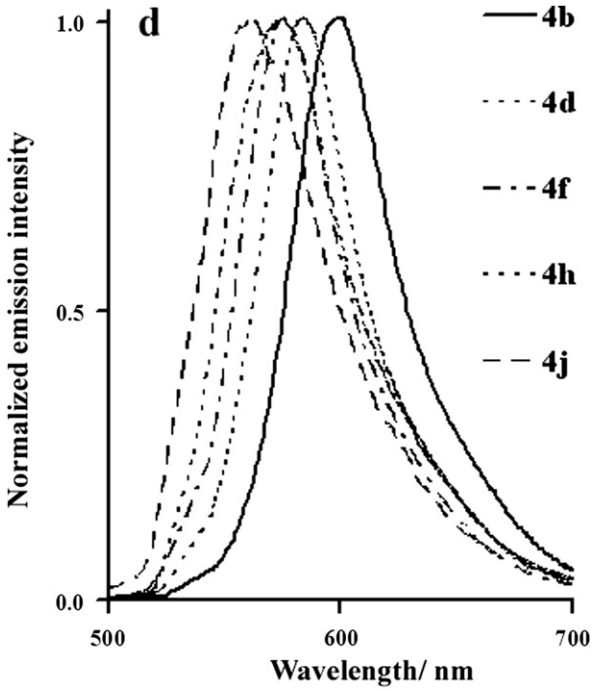

Fig. 6. Normalized fluorescence spectra for dyes **4b**, **4d**, **4f**, **4h**, and **4j** in dimethyl sulfoxide.

The introduction of polar substituents into organic chromophores causes a redistribution of the electron density in both the ground state and the excited state, which can strongly modify their absorption and fluorescence properties [25]. We also investigated the correlation between the polarization resonance effects of the electron withdrawing substitution on R^2 of dyes **4a**, **4c**, **4e**, **4g** and **4i** regarding their fluorescence and absorption maxima. Hammett substituent constants σ_p versus the fluorescence maxima of dyes were plotted and the results are shown in Fig. 7 [26]. The positive σ_p value due to a substituent and indicates an electron withdrawing polarization resonance effect of the group upon the conjugated system; all of the R^2 substituents in dyes **4a**–**j** have positive σ_p values. We observed a linear relationship between the polarization resonance effects of the electron withdrawing substitution on R^2 in dyes **4a**–**j** with their fluorescence maxima; as the σ_p value of the R^2 increased, the fluorescence maximum value of the dye shifted toward the red region of the spectra. The nitro group in **4a** and **4b**, which has the highest σ_p values of the substituents amongst all the dyes tested, induced the strongest electron withdrawing polarization resonance effects on the conjugated structure of the dyes; thus their fluorescence spectra exhibited the greatest red shift among the tested dyes with λ_{max} at ca 600 nm, while the others short of emission maxima value in the long-wavelength region. However, we did not observe the same linear relationship between the σ_p value of the R^2 dyes **4a**–**j** with

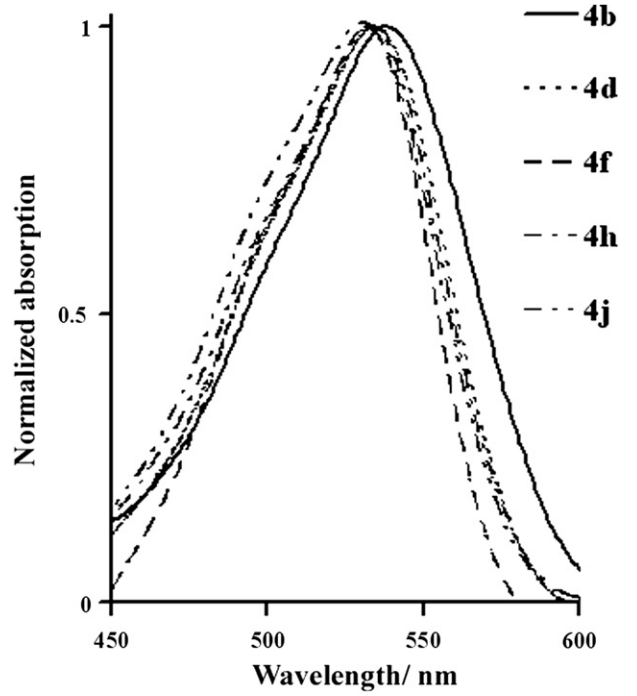

Fig. 5. Normalized absorption spectra for dyes **4b**, **4d**, **4f**, **4h**, and **4j** in dimethyl sulfoxide.

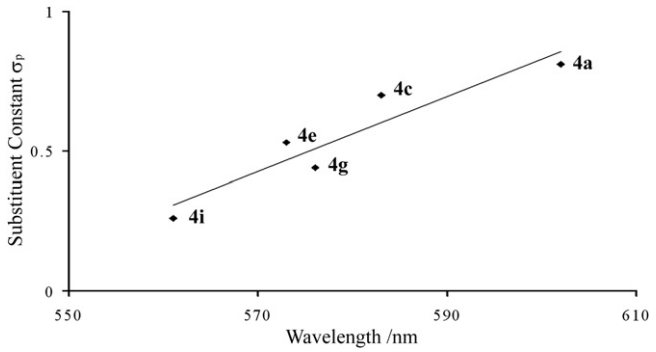

Fig. 7. Plot of Hammett substituents constant σ_p versus the fluorescence maxima for dyes **4a**, **4c**, **4e**, **4g**, and **4i**.

absorption maxima. To summarize, it can be concluded the R^2 substituent in dyes **4a**–**j** induced a redistribution of the electron density in both the ground state and the excited state resulting in shifting of the fluorescence maxima of the dyes toward to the long-wavelength region.

3.3. Spectral characteristics of the dyes *3*, *5*, *6*, and *7*

The spectral characteristics of dyes **3**, **5**, **6**, and **7**, such as the absorption maxima (λ_{max}) and emission maxima (λ_{em}) were also measured in DMSO, and the results are also presented in Table 1 and Figs. 8 and 9. In general, the absorption and fluorescence spectra characteristics and maxima for dyes **3**, **5**, **6**, or **7** were nearly identical for either the *N*-ethyl or *N*-butyl substitutions (Table 1). The electron absorption spectra of dye **3a** displayed an absorption in the visible region from 400 nm to 600 nm with an absorption maximum at 551 and a shoulder peak at 500 nm; the fluorescence spectra of dye 3a displayed an emission spectra in the visible region from 500 nm to 700 nm with an emission maximum at 577 nm (Figs. 8 and 9). We observed a small red shift in both the absorption maximum (20 nm) and fluorescence maximum (30 nm) as the π conjugation in **3a** was extended by incorporation of a 4-carboxybenzenesulfonyl moiety in **6a** (Table 1 and Fig. 9). The bathochromic effect of an electron-withdrawing nitrile at the 4-position in the chromene moiety is known in the chemistry of optical fluorophores derived from coumarin [24,27]. We observed a similar dramatic bathochromic shift in both the absorption (89 nm) and emission (112 nm) maxima as the 4 position of the chromene moiety in **3a** was substituted by an electron-withdrawing nitrile group in **5a** (Table 1 and Figs. 8 and 9). Finally, extending the π conjugation of **5a** with the 4-carboxybenzenesulfonyl moiety also resulted in a small red shift in both the absorption and emission maximum (Figs. 8 and 9). The dyes **7a** and **b** exhibited the longest absorption and emission maximum of the tested compounds, and they showed fluorescence in the NIR region of the spectrum.

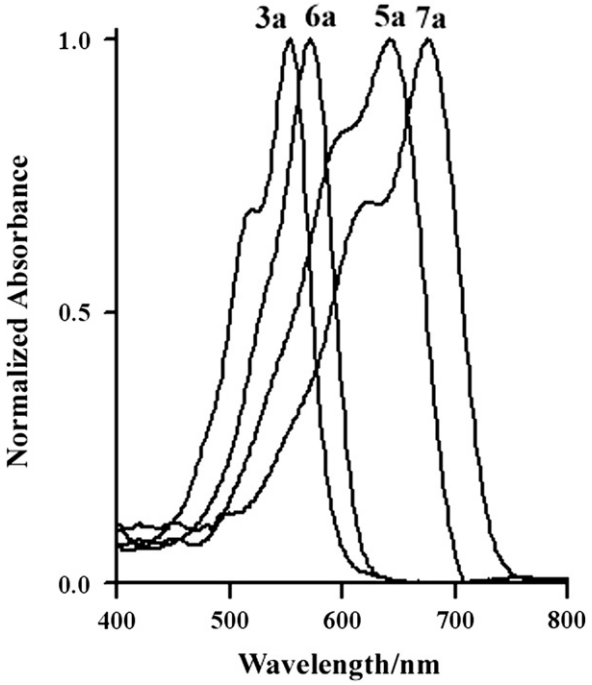

Fig. 8. Normalized absorption spectra for dyes **3a**, **5a**, **6a**, and **7a** in dimethyl sulfoxide.

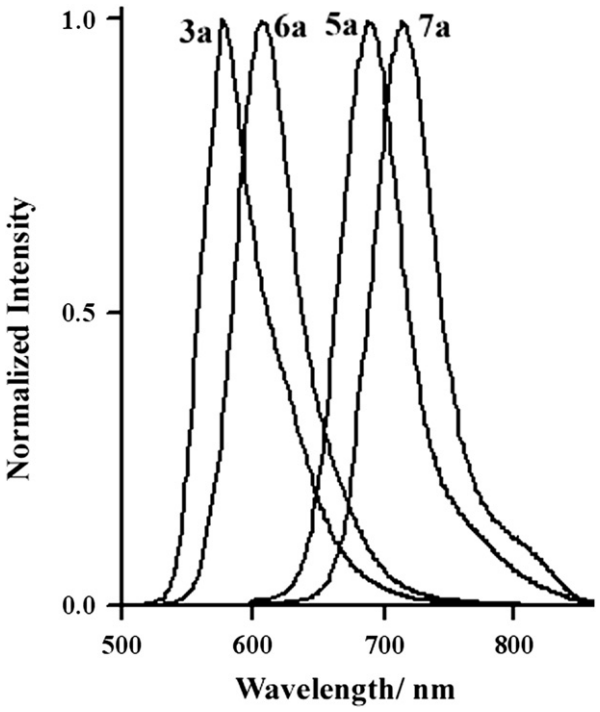

Fig. 9. Normalized emission spectra for dyes **3a**, **5a**, **6a**, and **7a** in dimethyl sulfoxide.

3.4. Extinction coefficient and quantum yield of dyes *3*, *4*, *5*, *6*, and *7*

The extinction coefficient (ε) and quantum yields (ϕ) of the dyes 3, 4, 5, 6, and 7 were measured in DMSO and the results are also summarized in Table 1. The dyes **4a**–**j** have retained the extinction coefficient values (35 658–61 802 M^{-1} cm^{-1}) as compared to coumarin **1**; however, dyes **4a**–**j** suffer a major fluorescence quench and their quantum yields ($\phi < 0.2$) are much lower than coumarin **1** (Table 1); thus, we are unable to rationalize this observation with the current experimental data. On the other hand, dyes **3**, **5**, **6**, and **7** are slightly less light absorptive with lower extinction coefficient values (12 842–41 160 M^{-1} cm^{-1}) as compared to coumarin **1** (Table 1). The dyes **3a**–**b** and **6a**–**b** have the highest quantum yields ($\phi > 0.84$) tested in this study; however, dyes **5a**–**b** and **7a**–**b**, which contain a nitrile group at the 4 position in the chromene moiety, exhibit low quantum yields as compared to analogue dyes **3a**–**b** and **6a**–**b**, respectively. We believe that the striking decrease in the quantum yields for **5a**–**b** and **7a**–**b** might be induced by the strong electron withdrawing nitrile substitution because a similar effect has also been observed in other coumarin derivatives [28]. The decrease in the fluorescence efficiency of various coumarin dyes has generally come to be accepted as due to charge transfer between the donor and acceptor moieties coupled with an internal twist in the excited state leading to a nonplanar twisted conformation with a large dipolar character which is known as the twisted intramolecular charge transfer (TICT) state [29]. The electron withdrawing nitrile substituents, especially at the 4-position of the chromene moiety in coumarin dyes further enhances charge separation, which markedly accelerates the population of the TICT state; therefore, 4-nitrile substituted coumarin dyes exhibited a low quantum yield [28]. We postulated that dyes **5a**–**b** and **7a**–**b** might exhibit the same effect as the coumarin dyes; therefore, dyes **5a**–**b** and **7a**–**b** exhibited low quantum yields. We are currently designing more experiments to rationalize the possible causes of inducing a low quantum yield for these synthesized dyes.

Table 2
Spectral properties of the dyes in different solvents.

Dyes	Dimethyl sulfoxide					Acetonitrile					Chloroform[a]				
	λ_{abs} (nm)	λ_{flu} (nm)	ε (M^{-1} cm^{-1})	Stokes shift	ϕ[b]	λ_{abs} (nm)	λ_{flu} (nm)	ε (M^{-1} cm^{-1})	Stokes shift	ϕ[b]	λ_{abs} (nm)	λ_{flu} (nm)	ε (M^{-1} cm^{-1})	Stokes shift	ϕ[b]
4a	536	600	56 667	64	8.8 E^{-3}	527	585	55 439	58	8.8 E^{-3}	531	578	50 146	47	7.8 E^{-3}
4c	532	580	61 802	48	5.4 E^{-3}	524	557	41 530	33	3.9 E^{-3}	529	540	41 646	11	4.5 E^{-3}
4e	530	573	60 544	43	6.5 E^{-3}	522	550	80 832	28	6.7 E^{-3}	526	541	61 901	15	5.8 E^{-3}
4g	531	581	47 428	50	3.8 E^{-3}	523	565	51 764	42	3.1 E^{-3}	527	561	58 826	34	3.8 E^{-3}
4i	529	561	42 869	32	3.2 E^{-3}	521	548	56 096	27	3.7 E^{-3}	525	541	56 232	16	3.5 E^{-3}
3a	551	577	23 498	26	0.92	544	568	25 184	24	0.93	551	562	34 453	11	0.92
5a	640	689	32 148	49	0.19	630	677	34 778	47	0.29	631	660	61 403	29	0.43
6a	570	607	18 128	37	0.90	565	603	20 019	38	0.91	–	–	–	–	–
7a	673	715	12 842	42	0.11	663	704	14 952	41	0.19	–	–	–	–	–

[a] Dyes **6a** and **7a** were in soluble in chloroform.
[b] Reference dyes are listed in the Experimental section.

3.5. *Effect of solvent polarity for dyes **3**, **4**, **5**, **6**, and **7***

The effect of the solvent polarity on the optical properties of the dyes synthesized in this study was investigated, because many fluorescent dyes are influenced by the solvent polarity, and their optical characteristics change (Table 2). All of the synthesized dyes exhibited small blue shifts along with a decreased solvent polarity (solvent polarity: DMSO > acetonitrile > chloroform), and optical characteristic of the coumarin dyes exhibited similar trends [30].

In terms of the quantum yields, dyes **4a**, **4c**, **4e**, **4g**, **4i** showed almost no fluorescence increase, and retained a low quantum yield in all of the tested solvent (Table 2). On the other hand, dyes **3a** and **6a** exhibited no change in the fluorescence quantum yield as the polarity of the solvent decreased. In contrast, dyes **5a** and **7a** showed an increased fluorescence quantum yield as the polarity of the solvent decreased. This fluorescence increase of **5a** and **7a** in less polar solvents is assumed to be due to the presence of the electron-donating moieties, which cause the TICT state. The TICT state is also known to influence the rate of nonradiative relaxation of the fluorophore, resulting in a diminished fluorescence quantum yield [29]. The TICT state is destabilized in the low polarity solvent; therefore, dyes **5a** and **7a** exhibited higher quantum yields in chloroform and acetonitrile, respectively, as compared to DMSO.

4. Conclusions

A series of novel iminocoumarin derived dyes **4**, **5**, **6**, and **7** have been designed and synthesized for application as long-wavelength fluorescent dyes by extending the π-conjugation and benzimidazole unit fixation of the benzimidazolic bicycle and iminochromene into a planar structure. The photophysical characterization showed that these iminocoumarin derived dyes are suitable for long-wavelength fluorescent dyes applications, and the dyes **7a** and **b** showed fluorescent maxima in the NIR region. The present molecular design based on the iminocoumarin moiety will enable the synthesis of a variety of dyes containing various functional groups, paving the way for the exploitation of new long-wavelength fluorescent dyes. We are currently modifying our design to optimize the quantum yield and also studying their cytotoxic effects in biological systems.

Acknowledgements

NSC grant 96-2113-M-027-002-MY3 and outstanding project on solar cell supported by National Taipei University of Technology is appreciated. We are also grateful to the National Center for High-performance computing for the computer time and facilities.

References

[1] Valeur B. Molecular fluorescence: principles and applications. Weinheim, Germany: Wiley-VCH; 2002.
[2] Betzig E, Patterson GH, Sougrat R, Lindwasser OW, Olenych S, Bonifacino JS, et al. Imaging intracellular fluorescent proteins at nanometer resolution. Science 2006;313(5793):1642–5.
[3] Rust MJ, Bates X, Zhuang X. Sub-diffraction-limit imaging by stochastic optical reconstruction microscopy (STORM). Nature Methods 2006;3(2):793–5.
[4] Jaiswal JK, Simon SM. Imaging single events at the cell membrane. Nature Chemical Biology 2007;3(2):92–8.
[5] Xie XS, Yu J, Yang WY. Living cells as test tubes. Science 2006;312(5771):228–30.
[6] Weissleder R. A cleaver vision for in vivo imaging. Nature Biotechnology 2001;19(4):316–7.
[7] Christie RM. Fluorescent dyes. Review of Progress in Coloration and Related Topics 1993;23:1–18.
[8] Alonso M-T, Brunet E, Juanes O, Rodrigues-Ubis J-C. Synthesis and photochemical properties of new coumarin-derived ionophores and their alkaline-earth and lanthanide complexes. Journal Photochemical Photobiology A 2002;147(2):113–25.
[9] Roussakis E, Liepouri F, Nifli A-P, Castanas E, Deligeorgiev TG, Katerinopoulos HE. ICPBC and C12-ICPBC: two new red emitting, fluorescent Ca^{2+} indicators excited with visible light. Cell Calcium 2002;3:221–8.
[10] Komatsu K, Urano Y, Kojima H, Nagano T. Development of an iminocoumarin-based zinc sensor suitable for ratiometric fluorescent imaging of neural zinc. Journal of the American Chemical Society 2007;129(44):13447–54.
[11] Vasylevska AS, Karasyov AA, Borisov SM, Krause C. Novel coumarin-based fluorescent pH indicators, probes and membranes covering a broad pH range. Analytical Bioanalytical Chemistry 2007;387(6):2131–41.
[12] Karasyov AA, Lukatskaya LL, Rubtsov MI, Sizova ZA, Doroshenko AO. Synthesis, acid-base and spectral properties of 3-(benzoimidazol-2-yl)-2-phenylimino-2H-chromenes. Russian Chemical Bulletin 2002;51(11):2070–3.
[13] Syzova ZA, Doroshenko AO, Lukatskaya LL, Rubtsov MI, Karasyov AA. Bichromophoric fluorescent dyes with rigid molecular structure: fluorescence ability regulation by the photoinduced intramolecular electron transfer. Journal of Photochemistry and Photobiology A: Chemistry 2004;165(1–3):59–68.
[14] Gorobets NY, Abakumov VV, Borisov AV, Nikitchenko VM. Novel aspects of the reaction of 3-(benzimidazol-2-yl)-2-iminocoumarins with aromatic aldehydes. Chemistry of Heterocyclic Compounds 2004;40(3):334–42.
[15] Maslov VV, Gorobets NY, Borisov AV, Nikitchenko VM. New series of dyes for flashlamp-excited lasers. Journal Applied Spectroscopy 2006;73(5):454–7.
[16] Kandavelu V, Huang HS, Jian JL, Yang TC-K, Wang KL, Huang ST. Novel iminocoumarin dyes as photosensitizers for dye-sensitized solar cell. Solar Energy 2009;83(4):574–81.
[17] Matsumoto S, Hattori R, Fukumaro K. Photosensitive lithographic printing plate with improved adhesion to support Japan patent, 1999, JP11024243A.
[18] Oonishi M. Coloring of Organic polymers with benzopyran derivatives Japan patent, 1994, JP06316649A.
[19] Moeckli P. Benzopyran dyes United States patent, 1985, US4547579A.
[20] Kühle E. Kohlensäurederivate aus formamiden. Angewante Chemie 1962;74:861–6.
[21] Umezawa K, Nakamura Y, Makino H, Citterio D, Suzuki K. Bright, color-tunable fluorescent dyes in the visible-near-infrared region. Journal of the American Chemical Society 2008;130(5):1550–1.
[22] Magde D, Brannon JH, Cremers TL, Olmsted J. Absolute luminescence yield of cresyl violet. A Standard for the Red Journal of Physical Chemistry 1979;83(6):696.

[23] Vincett PS, Voigt EM, Rieckhoff KE. Phosphorescence and fluorescence of phthalocyanines. Journal of Physical Chemistry 1971;55(8):4131–41.
[24] Wolfbeis OS, Koller E, Hochmuth P. The unusually strong effect of a 4-cyano group upon electronic spectra and dissociation constants of 3-substituted 7-hydroxycoumarins. Bulletin Chemical Society Japan 1985; 58:731–41.
[25] Griffith J. Color and constitution of organic molecules. London: Academic Press; 1976.
[26] Exner O. In: Chapman NB, Shorter J, editors. Correlation analysis in chemistry. New York: Plenum Press; 1978 [chapter 10].
[27] Gold H. In: Coulson F, Korte F, editors. Fluorescent whitening agents. Stuttgart: George Thiem Verlag; 1975.
[28] Bangar Raju B. Photophysical properties of ground-state twisted bicoumarins. Journal of Physical Chemistry A 1997;101(6):981–7.
[29] Grabowski ZR, Rotkiewicz K, Siemiarczuk A, Cowley DJ, Bauman W. Dual fluorescence of donor–acceptor molecules and the twisted intramolecular charge transfer (TICT) states. Journal of Luminescence 1979;18–19(part 1): 420–4.
[30] Peng MS, Cai J. Synthesis and fluorescence of crown ethers containing coumarin. Dyes and Pigments 2008;79(3):270–2.